Purinergic Signalling (2015) 11:551–560
DOI 10.1007/s11302-015-9473-4

ORIGINAL ARTICLE

Properties of ATP-gated ion channels assembled from $P2X_2$ subunits in mouse cochlear Reissner's membrane epithelial cells

Rachel T. Morton-Jones[1] · Srdjan M. Vlajkovic[1,2] · Peter R. Thorne[1,2,3] · Debra A. Cockayne[4] · Allen F. Ryan[5] · Gary D. Housley[6]

Received: 25 August 2015 / Accepted: 16 September 2015 / Published online: 1 October 2015

Abstract In the cochlea, Reissner's membrane separates the scala media endolymphatic compartment that sustains the positive endocochlear potential and ion composition necessary for sound transduction, from the scala vestibuli perilymphatic compartment. It is known that with sustained elevated sound levels, adenosine 5 -triphosphate (ATP) is released into the endolymph and ATP-gated ion channels on the epithelial cells lining the endolymphatic compartment shunt the electrochemical driving force, contributing to protective purinergic hearing adaptation. This study characterises the properties of epithelial cell $P2X_2$-type ATP-activated membrane conductance in the mouse Reissner's membrane, which forms a substantial fraction of the scale media surface. The cells were found to express two isoforms (a and b) of the $P2X_2$ subunit arising from alternative splicing of the messenger RNA (mRNA) transcript that could contribute to the trimeric subunit assembly. The ATP-activated conductance demonstrated both immediate and delayed desensitisation consistent with incorporation of the combination of $P2X_2$ subunit isoforms. Activation by the ATP analogue 2meSATP had equipotency to ATP, whereas α,β-meATP and adenosine 5′-diphosphate (ADP) were ineffective. Positive allosteric modulation of the $P2X_2$ channels by protons was profound. This native conductance was blocked by the $P2X_2$-selective blocker pyridoxalphosphate-6-azophenyl-2 ,4 -disulphonic acid (PPADS) and the conductance was absent in these cells isolated from mice null for the *P2rX2* gene encoding the $P2X_2$ receptor subunit. The activation and desensitisation properties of the Reissner's membrane epithelial cell ATP-gated $P2X_2$ channels likely contribute to the sensitivity and kinetics of purinergic control of the electrochemical driving force for sound transduction invoked by noise exposure.

Keywords ATP-gated ion channel · P2X receptor · Cochlea · Mouse · Desensitisation · Splice variants · Knockout · *P2rX2* gene · Purinergic receptor pharmacology · Hearing

✉ Gary D. Housley
g.housley@unsw.edu.au

[1] Department of Physiology, University of Auckland, Auckland, New Zealand

[2] Centre for Brain Research, School of Medical Sciences, University of Auckland, Auckland, New Zealand

[3] Section of Audiology, School of Population Health, University of Auckland, Private Bag 92019, Auckland, New Zealand

[4] Boston Scientific, San Jose, CA 95134, USA

[5] Departments of Surgery and Neurosciences, VA Medical Center, University of California San Diego, La Jolla, CA 92037, USA

[6] Translational Neuroscience Facility and Department of Physiology, School of Medical Sciences, UNSW Australia, Sydney, NSW 2052, Australia

Introduction

P2X receptors are membrane ion channels activated by the binding of extracellular adenosine 5 -triphosphate (ATP). Seven P2X receptor subunits have been identified, which form either homomeric or heteromeric channels and give rise to a wide range of phenotypes dependent on the trimeric subunit assembly of the channel [1–3]. The functional classification of P2X receptors has usually been based on the time course and pharmacological profile to agonists and antagonists. Many recognised properties of P2X receptors are based on data from recombinant channels, expressed heterologously in either oocytes or mammalian cells (for review, see [4]). However, in

native cells, attribution of the functional molecular subtype has been more difficult, due to the potential for multiple P2X receptor subtypes to be expressed, including splice variants and a lack of selective pharmacological modulators for many of the P2X receptor subtypes. Molecular approaches, such as using knockout mice, antisense and interference RNA have been used to substantiate the role of particular P2X receptor subunits in native cell purinergic signalling phenotypes.

Given that $P2X_2$-like receptor action dominates purinergic signalling in the cochlea (for reviews, see [5, 6]), this sensory organ offers an excellent model to characterise the phenotype and molecular profile of native $P2X_2$-type ATP-gated ion channels. In the cochlea, ATP influences sound transduction, the endocochlear potential and neurotransmission, and underlies an intrinsic purinergic $P2X_2$ receptor-based humoral hearing adaptation mechanism that reduces hearing sensitivity as sustained sound levels increase [7]. However, native ATP-induced responses in many cochlear cells have not correlated well with known recombinant P2X receptor combinations [8–13]. This has been mainly attributed to heteromeric expression, with multiple $P2X_2$ splice variant combinations possible [14–16], as demonstrated in rat primary auditory neurons expressing a novel $P2X_{2-3}/_3$ heteromer [17]. Such has been the case for the P2X receptor in Reissner's membrane (RM), a two-cell-thick partition that separates the endolymphatic (high K^+, low Na^+) and perilymphatic (high Na^+, low K^+) fluid compartments. $P2X_2$ expression has been detected in guinea pig, rat and mouse RM, although electrophysiological recordings in guinea pig RM indicated additional subunits, assembling as heteromeric receptors [8]. P2X receptor in RM are considered to provide a current path between the endolymphatic and perilymphatic compartments in the cochlea, which would limit the driving force for sound transduction [6].

We have previously reported that the ATP-gated conductance in the cochlear partition arising from a range of epithelial cells facing scala media (endolymphatic compartment) was absent in the *P2rX2* null mouse [7]. Whole-cell patch clamp analysis showed that the sustained inward currents elicited by ATP application was absent from $P2rX2^{-/-}$ inner and outer hair cells as well as RM epithelial cells, indicating that this conductance arose from a homomeric $P2X_2$ trimeric subunit configuration of the ATP-gated ion channels. Extending from this, the *P2rX2* null mouse also lacked the extracellular fall in endocochlear potential and associated decrease in cochlear partition resistance that is evident when picolitres of ATP is injected into the endolymphatic compartment [7]. This finding suggests that all of the ATP-activated membrane conductance in cell lining that cochlear compartment is attributable to $P2X_2$-type channels. *P2rX2* null mice also had a distinct hearing phenotype, in which sustained elevation of sound levels failed to elicit the temporary reduction in hearing threshold (temporary threshold shift) which occurs with wild-type (WT) mice. With supra-physiological sound levels, *P2rX2* null mouse developed permanent hearing loss. This $P2X_2$ receptor-based purinergic hearing adaptation therefore provides protection from noise-induced hearing loss [7]. Analysis of long-term moderate environmental noise exposure, or ageing, further indicated that the $P2X_2$ receptor-based hearing adaptation mechanism contributes to otoprotection across a lifetime [18]. These findings together indicate that $P2X_2$ receptors are the first stage in a purinergic hearing adaptation mechanism which provides autocrine and paracrine regulation of sound transduction and auditory neurotransmission. Given that several mutations in the *P2rX2* gene encoding the $P2X_2$ receptor have now been shown to contribute to human hearing loss, including DFNA41 autosomal dominant progressive hearing loss [18, 19] and a mitochondrial (MELAS)-associated hearing disorder [20], knowledge of $P2X_2$ receptor function has considerable health relevance.

The above data highlight the importance of understanding the substrates of cochlear purinergic signalling, which could inform future otoprotective strategies. Here, we provide a characterisation of the native $P2X_2$ receptor type ATP-gated ion channels expressed by mouse cochlear Reissner's membrane epithelial cells. We show evidence for alternative splicing of the messenger RNA (mRNA) transcripts and show that these homomeric $P2X_2$-type channels exhibit relatively fast desensitisation properties relative to the known kinetics of $P2X_2$ receptor subunits studied in heterologous expression systems.

Materials and methods

Animals

Experiments were performed on cochlear tissue obtained from 8- to10-week-old mice (C57BL/6J strain) euthanized by intraperitoneal injection of sodium pentobarbitone (100 mg/kg; Pentobarbital 300; National Veterinary Supplies Ltd., Auckland, New Zealand). *P2rX2* null mice encoding the ATP-gated ion channel $P2X_2$ subunit (Roche Palo Alto, CA, USA; [21]) provided a control for background membrane conductance. The *P2rX2* null mouse colony founders were all genotyped using a DNeasy blood and tissue kit (QIAGEN, New Zealand) and previously described PCR primers [21] to confirm the absence of the *P2rX2* gene (data not shown). All experiments were approved by the animal ethics committees of the University of Auckland (New Zealand) and the University of Cambridge (UK).

Reverse transcription-polymerase chain reaction

RM was carefully microdissected in filtered artificial perilymph solution (in mM: NaCl, 150; KCl, 4; Na_2HPO_4, 8;

NaH_2PO_4, 2; $CaCl_2$, 1.5; $MgCl_2$, 1; D-glucose, 10; pH 7.25 with NaOH; osmolarity, 320 mOsm/l) from the cochleae of 4 mice in three independent experiments (total of 12 mice). Whole cochlear tissue (two samples) was also evaluated. Total RNA was extracted from the whole cochlea and microdissected RM tissue samples using TRIzol™ Reagent. A sample of the artificial perilymph dissection solution was processed alongside as a control. First-strand complementary DNA (cDNA) synthesis was carried out using 5 μl total RNA as template in a 20-μl reverse transcription (RT) reaction using a SuperScript™ III First-Strand Synthesis SuperMix kit primed with random hexamers. Mouse $P2X_2$ receptor-specific primers were used to amplify $P2X_2$ cDNA; sense primer 5′-CGGGGTGGGCTCCTTTCTGT-3′; antisense primer 5′-GGACATGGTTACTGAAGAGCG-3′, corresponding to positions 1318 and 1816 bp of the $P2X_2$ cDNA mouse sequence (GenBank accession #NM153400) and resulting in a predicted 499 bp PCR product. Equivalent primers have been successfully used to detect $P2X_2$ cDNA splice variants in rat and guinea pig cochlear tissue [8, 17, 22]. A 25-μl PCR reaction contained 2 μl of the RT reaction as cDNA template, 1 unit Platinum® *Taq* DNA polymerase, 1× PCR buffer, 2 mM $MgCl_2$, 0.2 mM dNTPs, and 0.2 μM primers. cDNA was denatured to 94 °C for 5 min before using a 25 thermal cycle profile of 94 °C for 45 s, 60 °C for 45 s and 72 °C for 90 s, followed by a final extension at 72 °C for 10 min. This PCR reaction was re-amplified in a second PCR reaction using 2 μl of the first PCR reaction as template for a further 30 cycles using the same thermal profile. Control reactions included no reverse transcriptase in the RT reaction (total RNA included) to preclude possible genomic contamination, and a no template control (total RNA omitted in RT reaction) to confirm the absence of cross contamination. A positive control DNA template was also included using previously cloned $P2X_2$ receptor cDNA (not shown) [17]. The resulting PCR cDNA products were extracted from agarose gel, purified using a QIAquick gel extraction kit (QIAGEN, New Zealand), and sequenced using a ABI 373A sequencer (Applied Biosystems). All products were obtained from Invitrogen, New Zealand unless stated otherwise.

Isolation of RM epithelial cells in situ

Cochleae were dissected in artificial perilymph solution. The bone (otic capsule) surrounding the cochlea was removed and the lateral wall peeled off to leave a sheet of RM attached to the spiral limbus. The spiral limbus was lifted off and removed from the central modiolus in three rough segments, approximating the apical, middle and basal turns.

Whole-cell voltage clamp

Spiral limbus segments with the sheets of attached RM were placed in a recording chamber on an upright microscope (Axioskop, Zeiss, Germany) and superfused with artificial perilymph solution. Cells were visualised using Normarski differential interference contrast optics and infrared video microscopy (Fig. 1a). Recording pipettes (2–5 MΩ; filamented borosilicate glass, Harvard apparatus, UK) were filled with the following internal solution (mM): KCl, 150; $MgCl_2$, 2; Na_2HPO_4, 8; NaH_2PO_4, 1; D-glucose, 3; $CaCl_2$, 0.001; EGTA 0.5; pH 7.25 with KOH; osmolarity, 320 mOsm/l. Whole-cell patch clamp recordings were made in situ using a patch clamp amplifier (Axopatch 200B, Axon Instruments, USA) controlled by pClamp9.2 software and digitised with a Digidata 1322 series interface (Axon Instruments, USA). The holding potential in all cells was −60 mV. Voltage errors due to series resistance were either compensated 85 % online or corrected during analysis. ATP-gated inward current desensitisation kinetics were fitted with a single exponential function by iterative best fit procedures. Dose-response data were fitted with sigmoidal functions to provide EC_{50} values (SigmaPlot 10). Data was analysed for normality using a Shapiro-Wilk normality test (OriginPro 7.5, OriginLab, USA). Data are presented as mean±S.E.M. Statistical significance was assessed using either analysis of variance (ANOVA; OriginPro 7.5, OriginLab, USA) or Student's *t* test where appropriate ($P<0.05$ significant).

Drugs and solutions

Adenosine 5′-triphosphate (ATP), and related analogues, 2-methylthioATP (2-meSATP; Calbiochem, USA), alpha, beta-methylene ATP (α,β-meATP) and adenosine 5′-diphosphate (ADP) were applied by pressure pipette. The P2X-selective antagonist pyridoxal-phosphate-6-azophenyl-2′,4′-disulphonic acid (PPADS) was applied by bath superfusion. All experiments were performed at room temperature (20–25 °C). Reagents were obtained from Sigma-Aldrich (New Zealand) unless stated. Drugs were prepared as aqueous stock solutions (stored at −20 °C) and diluted to final concentrations in artificial perilymph solution.

Results

RT-PCR analysis of $P2X_2$ receptor expression in mouse RM and whole cochlea resulted in the detection of two different $P2X_2$ cDNA amplicons at 499 and 293 bp (Fig. 1b). The 499-bp PCR product was the full-length $P2X_2$ ($P2X_{2-1}$; P2X2a; NM153400). The 293-bp PCR product was the $P2X_{2-2}$ (P2X2b; AB094664) splice variant previously detected in guinea pig and rat cochlea [15, 16, 22] with a 207-bp deletion

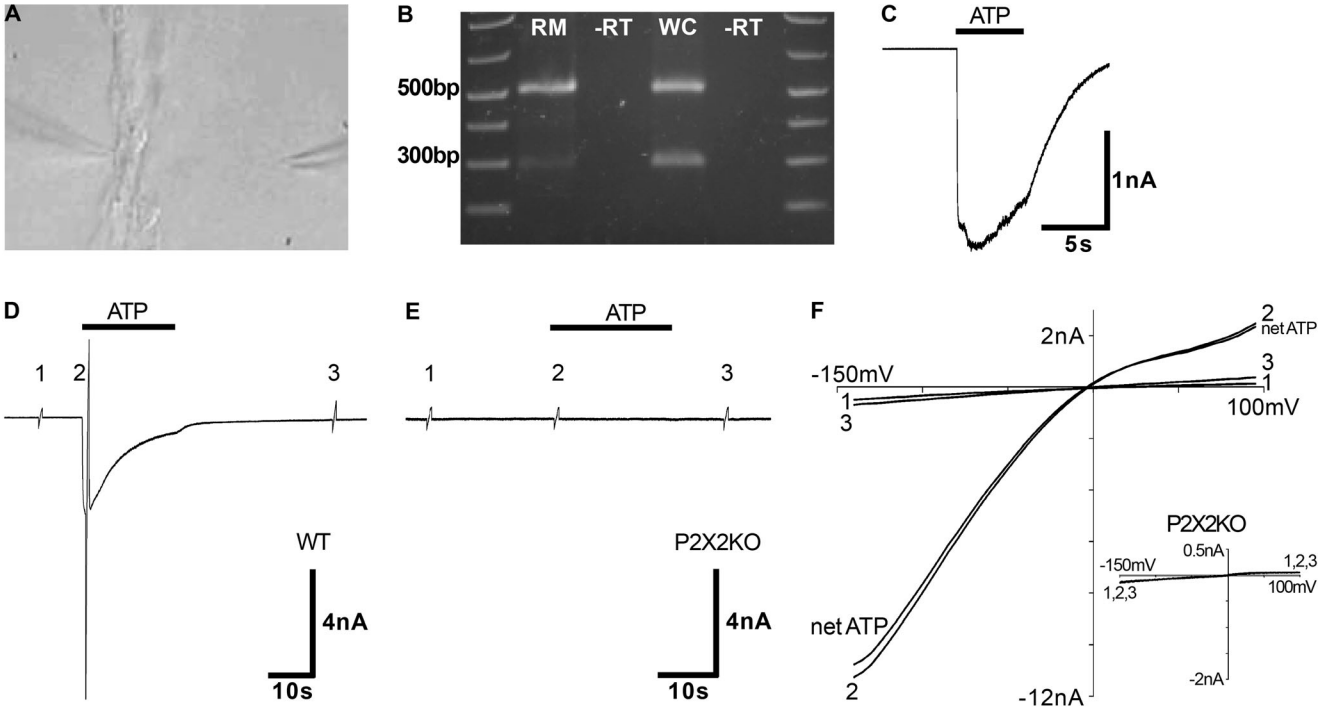

Fig. 1 Reissner's membrane (RM) epithelial cell $P2X_2$ mRNA and $P2X_2$-sepecific ATP-gated inward currents. **a** Image showing whole-cell voltage clamp recording from an epithelial cell in situ. **b** Agarose gel (1.5 %) showing full-length P2X2a and splice variant P2X2b cDNAs derived from RM and whole cochlea (*WC*) mRNA. Predicted RT-PCR product sizes are 499 bp for full-length P2X2a and 293 bp for P2X2b. –RT (control) indicates omission of reverse transcriptase. *Left and right lanes* are loaded with 1 kb plus DNA ladder. **c** 100 μM ATP evoked a fast inward current in wild-type RM epithelial cells. *Horizontal bar* above response indicates the ATP application period. **d** Record of the current displacements during voltage ramps (−150 to +100 mV, 0.78 s) before (1), during (2) and after (3) ATP application in a wild-type RM epithelial cell. **e** ATP-induced current responses were not detected *P2rX2* null mouse RM epithelial cells, as demonstrated by the absence of current displacement during voltage ramps with ATP; before (1), during (2) and after (3) ATP application. **f** Current-voltage relationship for the ATP-induced current from **d**. The net ATP-activated conductance was derived by subtracting the current - voltage response immediately preceding the ATP application (1) from the peak current - voltage response during ATP (2). Note the inward rectification of the ATP-activated conductance. *Inset* displays the current-voltage relationship derived from **e** demonstrating the absence of ATP-induced currents in *P2rX2* null mouse RM epithelial cells

in the C-terminal region. These results were confirmed by sequencing and alignment with the published mouse sequences. The specificity of these results were confirmed by the inclusion of multiple negative controls; omission of reverse transcriptase (−RT) and of the RNA template (not shown), excluding amplification of genomic DNA and contamination. Analysis of the comparative intensity between the full-length P2X2a and P2X2b agarose gel electrophoresis separated PCR bands amplified from RM cDNA showed a 65.9± 4.2 % (n=14; P<0.00001; Student's paired t test) reduced intensity for the P2X2b splice variant cDNA (293 bp compared to 499 bp; Fig. 1b). A similar result was also seen for the PCR bands amplified from whole cochlea cDNA; P2X2b cDNA showed a 68.1±5.0 % (n=5; P<0.01; Student's paired t test) reduced intensity in comparison to the full-length $P2X_2$ cDNA. This suggests that the P2X2b transcript may be less abundant than the full-length $P2X_2$ transcript in both mouse RM and more broadly, within the whole mouse cochlea.

Whole-cell voltage clamp analysis was performed to functionally characterise the ATP-gated ion channels in RM epithelial cells of the mouse. Then, 100 μM ATP produced a rapid onset inward current in all RM epithelial cells that were tested, with an average peak current amplitude of −2.06± 0.17 nA (n=63; Figs. 1c, 3b). The background conductance in the RM epithelial cells was typically linear and the cells had a resting membrane potential (V_z), determined by voltage ramp (−150 to +100 mV, 0.8 s), that averaged −0.51± 1.00 mV (n=188; Fig. 1d, f). This is consistent with the predominance of voltage-insensitive stretch-activated non-selective cation channels and chloride channels which have been detected in guinea pig RM epithelial cells [23]. Series resistance related to pipette access was 5.3±0.1 MΩ, cell membrane capacitance (C_m) was 5.6±0.1 pF and average input resistance (R_m) was 423.4±37.2 MΩ, calculated from the current response to a −10 mV voltage step from a holding potential of −60 mV (equivalent to that reported in guinea pig [8]). Fig. 1d displays voltage ramps (−150 to +100 mV, 0.8 s) before (1), during (2) and after (3) an ATP-induced current response, with Fig. 1f displaying details of the resulting current-voltage relationship. The ATP-induced current displayed pronounced inward rectification and had a reversal potential on average of −6.37±1.09 mV (n=18)

(Fig. 1f), reflecting the relative lack of cation selectivity. In comparison, the adjacent RM mesenchymal cells on the opposing surface facing scala vestibuli did not respond to ATP (100 μM; $n=5$); consistent with the absence of $P2X_2$ immunolabelling reported for guinea pig mesenchymal cells [8]. The membrane properties of these mouse RM mesenchymal cells were V_z −20.2±4.9 mV; C_m 8.7±0.8 pF; R_m 639.6±209.1 MΩ; with outward rectification evident positive to ~−30 mV in voltage ramps (data not shown).

P2rX2$^{-/-}$ null mice were utilised as a control to characterise the underlying RM epithelial cell membrane conductance with ATP application (100 μM). No ATP-activated current response was detectable ($n=17$; Fig. 1e, f, inset), as reported previously [7]. Figure 1e displays voltage ramps (−150 mV to +100 mV, 0.8 s) in a *P2rX2*$^{-/-}$ null mouse RM epithelial cell before (1), during (2) and after (3) ATP application, with Fig. 1f inset displaying the resulting current-voltage relationship. Analysis of the membrane resistance about −60 mV in these cells (601.3±184.1 MΩ) showed no significant difference from that of the WT cells ($P=0.36$ compared with WT; unpaired *t* test). These results confirm that ATP-gated ion channels in RM epithelial cells are assembled as homomeric $P2X_2$ receptors and that knockout of the *P2rX2* gene did not induce compensation by other P2X subunits or alter other aspects of the membrane conductance.

The ATP-gated current responses showed progressive desensitisation in the peak current response upon repeated applications of 100 μM ATP (Fig. 2a). Recovery in the peak current response was demonstrated by increasing the interval between ATP applications. Comparable peak inward current responses were consistently obtained with short, 5-s pressure applications of ATP (100 μM) with 5-min washout in between ($n=8$; one-way ANOVA; Fig. 2b, c). The initial ATP-induced current responses exhibited some desensitisation in the presence of ATP (Fig. 2b); the fraction of current remaining at the end of the ATP application was 68.9±6.8 % ($n=8$; ATP1 at 5 s; Fig. 2g). Subsequent ATP-induced current responses delayed by 5 min to produce comparable peak inward currents desensitised significantly faster than the initial responses (Fig. 2b, c, g). The fraction of current remaining at the end of these second 5-s ATP applications was 37.6±10.1 % ($n=8$; $P<0.01$; Student's paired *t* test). A more prolonged (20 s) application of ATP (100 μM) demonstrated significant desensitisation during the first ATP response, with only 16.9±2.2 % residual at the end of the ATP application ($n=7$; ATP1 20 s; Fig. 2d). A second ATP-induced current response 5 min later showed very little recovery, with the average peak response only 27.3±5.2 % of the initial response ($n=7$; $P<0.001$; Student's paired *t* test; ATP2 20 s; Fig. 2d, f). This was only a little above the 16.9±2.2 % residual current at the end of the first response (Fig. 2d). However, when the second 20 s ATP-induced current response (2) was normalised to the first (1), it was found that the second current response consistently desensitised much faster in the presence of ATP (Fig. 2e). The fraction of current remaining at the end of the second ATP application (ATP2 at 20 s) was 6.5±1.8 %, compared to 16.9±2.2 % from the first (ATP1 at 20 s; $n=7$; $P<0.01$; Student's paired *t* test; Fig. 2g). The rate of desensitisation was examined by fitting a single exponential decay function to the current record, as displayed in Fig. 2e (dots). Figure 2h displays the desensitisation time constants (tau) for each cell (paired data), along with the mean data. The average tau value for initial current responses to ATP (20 s) was 7.8±1.1 s ($n=7$; Fig. 2h). This time constant was similar to that for guinea pig RM epithelial cells, which was 9.7±9.0 s [8]. The time constant for subsequent ATP responses, however, decreased by 64 % to 2.9±0.8 s ($n=7$; $P<0.01$ compared with the first response; Student's paired *t* test; Fig. 2h), signifying faster desensitisation kinetics with successive applications of ATP. These results indicate that there are two aspects to the desensitisation of native homomeric $P2X_2$ receptors in RM epithelial cells: (1) duration-dependent desensitisation of consecutive peak current amplitudes and (2) desensitisation triggered by ATP, which is less dependent upon duration of application and affects the rate of desensitisation in subsequent applications.

The functional classification for P2 receptor subtypes is usually based on the potency of P2 receptor agonists such as α,β-meATP and 2meSATP (for review, see [24]). These agonists were used at equimolar concentration (100 μM) to pharmacologically verify a $P2X_2$ receptor-like profile in RM epithelial cells. The ATP analogue 2meSATP (100 μM) elicited inward currents of −1.7±0.3 nA ($n=7$), which were not significantly different to 100 μM ATP (one-way ANOVA; Fig. 3a, b); 100 μM α,β-meATP ($n=5$), a potent $P2X_1$ and $P2X_3$ receptor agonist, and ADP ($n=5$), a $P2Y/P2X_1$ receptor agonist, did not generate detectable inward currents (Fig. 3a, b). Pre-incubation with the P2X receptor-selective antagonist PPADS for 5 min significantly inhibited initial ATP-induced currents by 75 % to 0.5±0.1 nA ($n=6$; $P<0.01$; Student's paired *t* test; Fig. 3c, d). In control conditions, comparable peak inward current responses were obtained to consecutive ATP applications (Fig. 2b, c). One property that differentiates $P2X_2$ receptors from all other homomeric P2X receptors is the ability of acidic pH to potentiate ATP-induced currents (for review, see [25]). Here, we examined the sensitivity of the ATP-induced current responses in RM epithelial cells to changes in pH by obtaining dose-response relationships for ATP at pH 7.25 and 6.25. Dose-response curves for ATP at these two pH values were obtained from first responses only due to the observed desensitisation. The maximum current response at pH 6.25 was 2.19±0.39 nA with 30 μM ATP, and at pH 7.25 was 2.06±0.17 nA with 100 μM ATP. These maximum responses were not significantly different ($P>0.05$; one-way ANOVA). The data were normalised to the maximum currents evoked by ATP and fitted with sigmoidal

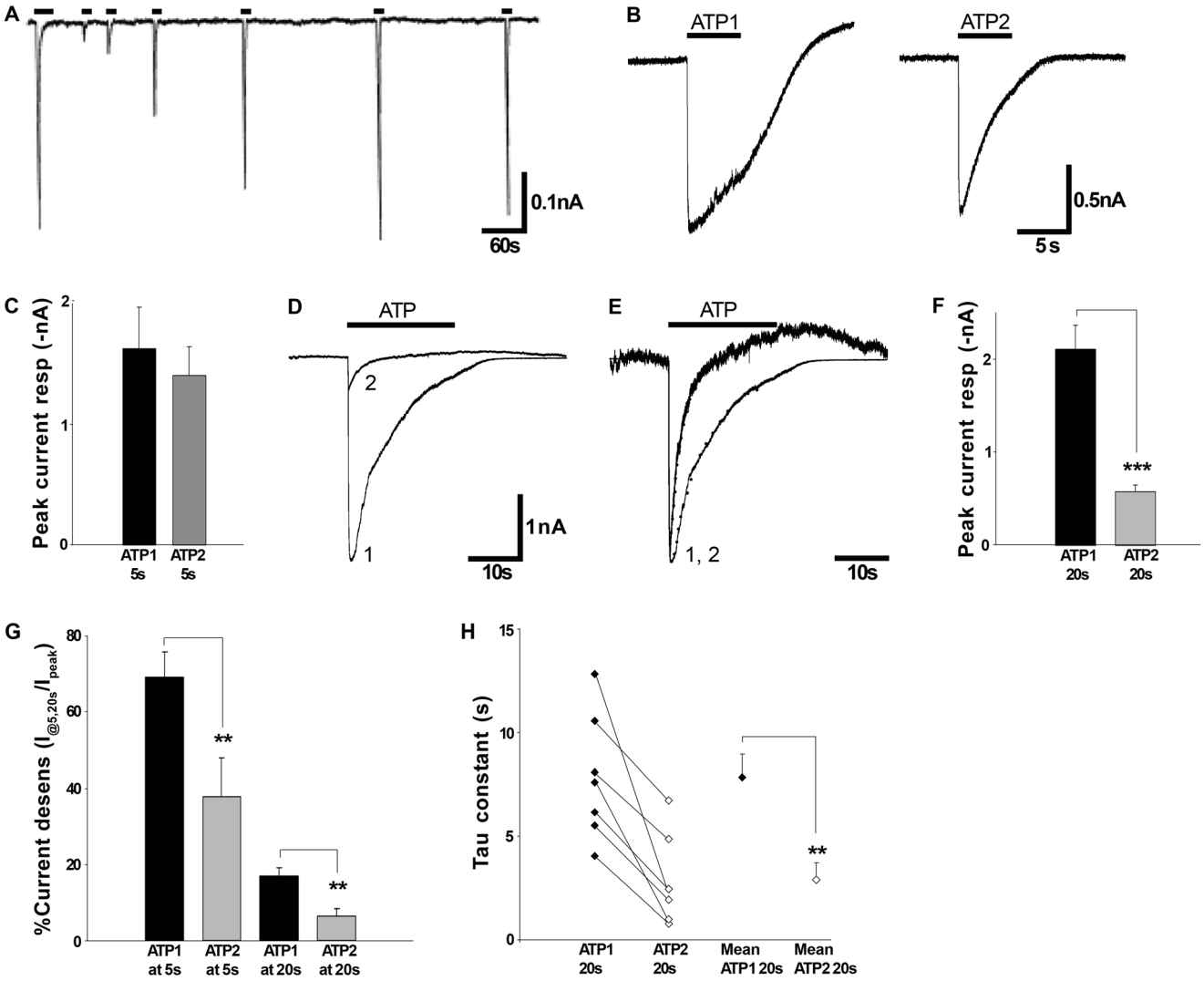

Fig. 2 Properties of the RM ATP-gated $P2X_2$ membrane conductance. **a** Repeated ATP (100 μM) applications progressively reduced the peak amplitude of the ATP-gated inward current, which recovered with increasing intervals between applications. Horizontal bars above responses indicate ATP application period. **b** 5 s ATP application activated fast inward currents that slowly desensitised in the presence of ATP (ATP1). Subsequent applications (ATP2) separated by 5-min activated comparable peak current responses but displayed significant desensitisation during ATP application. **c** *Bar graph* of the average response from **b** displaying comparable peak ATP-induced current responses (ATP1 and ATP2; $n=8$). Data represents mean±S.E.M. **d** More prolonged ATP applications (20 s; *1*) evoked relatively fast desensitising ATP-induced current responses. A second ATP application (*2*) 5 min later displayed significantly reduced peak ATP-induced current responses; first current response (*1*) is superimposed on the second current response (*2*). **e** Normalisation of the second current response from **d** to the first current response demonstrated significantly faster desensitisation in second ATP-induced current responses when compared to the first. **f** *Bar graph* of the average peak current responses from **d** (***$P<0.001$). **g** *Bar graph* of the fraction of current remaining at the end of consecutive 5 or 20 s ATP applications when compared to the peak response (**$P<0.01$; percentage %). **h** Scatter plot of desensitisation time (tau) constants for first (*closed diamonds*) and second (*open diamonds*) ATP applications ($n=7$). Paired data connected with lines. Average time constants±SEM were displayed on the *right-hand side* (**$P<0.01$)

dose-response curves to obtain EC_{50} values of 27.4 and 9.7 μM for pH 7.25 and 6.25, respectively (Fig. 3e). Acidification to pH 6.25 produced a leftward shift in the dose-response curve, with the ATP responses at pH 6.25 being significantly greater than the responses at pH 7.25 for ATP concentrations 4 μM - 30 μM ($P<0.0001$; two-way ANOVA). This pharmacological profile is consistent with $P2X_2$ receptor expression in RM epithelial cells.

Discussion

Here, we describe a native homomeric $P2X_2$ receptor expressed in the mouse cochlea which displays comparatively rapid desensitisation with unique properties.

Electrophysiological studies in P2X knockout mice have helped to assign the molecular composition of P2X receptors and their functional characterisation in native tissue [21]. In

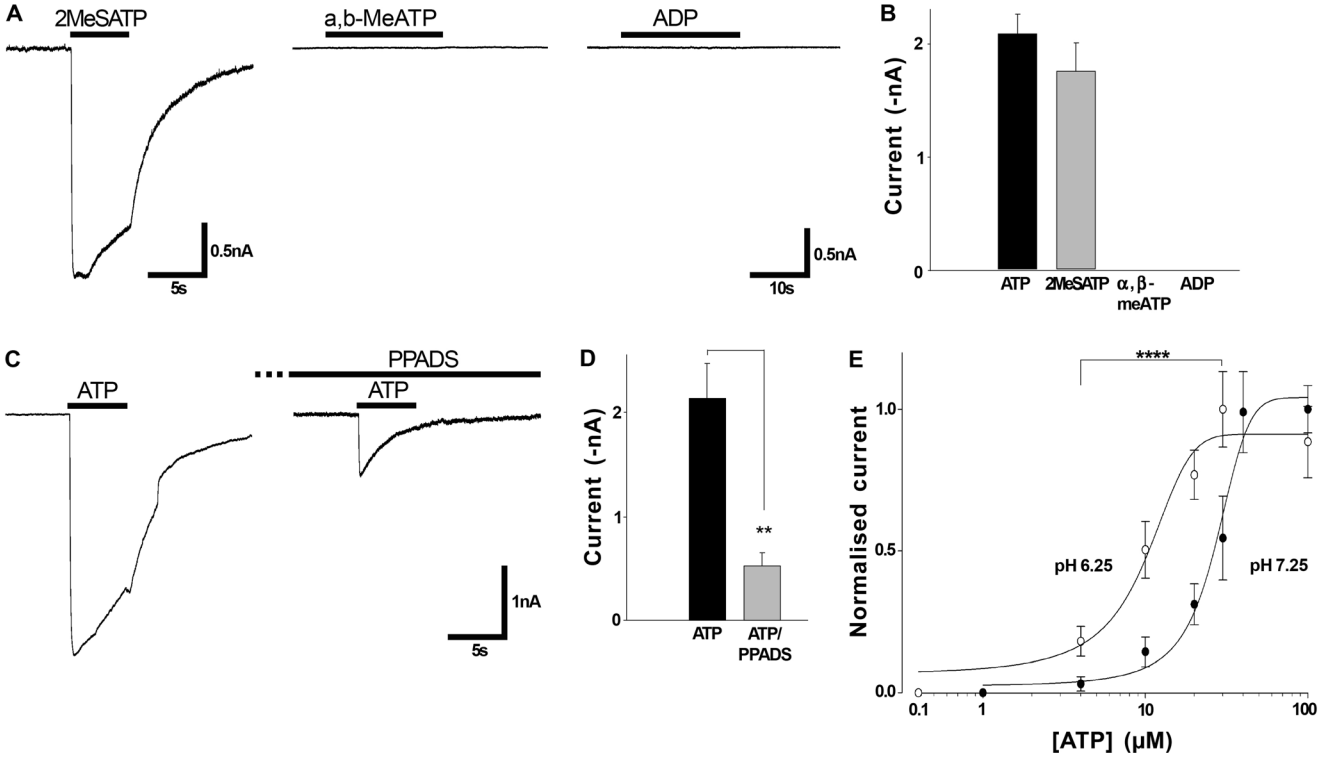

Fig. 3 Pharmacological profile of native RM epithelial cell $P2X_2$ receptors. **a** P2 receptor agonist-induced inward currents at equimolar concentrations. 100 μM 2meSATP (5 s) activated a fast inward current, whereas neither α,β-meATP (20 s) nor ADP evoked a response. *Horizontal bars* above responses indicate agonist application period. **b** *Bar graph* of the average peak current response by P2 agonists. Data represents mean±S.E.M. **c** ATP-activated inward currents were suppressed by pre-incubation of 10 μM PPADS for 5 min between ATP applications (indicated by *dotted lines*). **d** *Bar graph* of the average block of ATP-activated currents by 10 μM PPADS ($n=6$; ** $P<0.01$). **e** Dose-response relationships for currents activated by ATP at pH 7.25 (*closed circles*) and pH 6.25 (*open circles*), demonstrating potentiation of ATP-activated currents by acidification (4–30 μM ATP; ****$P<0.0001$; two-way ANOVA). Data were normalised to the maximum responses and displayed as mean±SEM. The EC_{50} at pH 7.25 and 6.25 were 27.4 and 9.7 μM, respectively

this study, absence of the $P2X_2$ receptor subunit completely eliminated all ATP-induced current responses in RM epithelial cells, demonstrating homomeric $P2X_2$ receptor functionality of the wild-type mice. A $P2X_2$ receptor-like pharmacological profile was obtained in wild-type RM epithelial cells in response to various P2 receptor agonists and antagonist, along with confirmation of the $P2X_2$-specific sensitivity to changes in pH. The pharmacological profile of the mouse RM ATP-induced currents were comparable to those from guinea pig RM epithelial cells, except for the absence of a response to α, β-meATP as reported for the guinea pig [8].

The high input resistance of the cells and the dominance of stretch-gated channels and chloride channels [8, 23], in the absence of $P2X_2$ receptor activation, reflects the role of RM in maintaining the electrochemical division between endolymph and perilymph. Loud sound is known to elevate ATP in the cochlear fluids and to result in a K^+ shunt conductance through P2X receptors in the epithelial cells of this compartment. This reduces hearing sensitivity by a reduction in the endocochlear potential [5, 26]. Given the significant surface area of RM, this tissue has the potential to mediate a large proportion of the P2X receptor-mediated decline in the endocochlear potential [7].

Traditionally, homomeric $P2X_2$ receptors characterised in heterologous expression systems exhibited only slow rates of desensitisation [1, 27], unlike $P2X_1$ and $P2X_3$ receptor subunits, which desensitise within milliseconds [1, 27]. The majority of heterologous expression studies of $P2X_2$ receptors report none or slow (tens of seconds) desensitisation; however, it is evident that alternative splicing influences this, along with expression level, cell type and experimental conditions [1, 17, 27, 28]. A feature of this native mouse RM epithelial cell $P2X_2$ receptor was its desensitisation properties. These consisted of two aspects; the first is typical of other P2X receptor studies, where duration-dependent desensitisation of consecutive peak current amplitudes developed following repeated ATP applications (Fig. 2a). A second form of desensitisation was triggered by ATP, which was less dependent upon duration of application and affected the rate of desensitisation in subsequent applications. Thus, consecutive applications of ATP in mouse RM epithelial cells triggered significantly faster desensitisation kinetics in subsequent

ATP-induced current responses (Fig. 2). The rate of desensitisation for initial ATP responses had a time constant of ~8 s, which was generally comparable to guinea pig RM epithelial cells (~10 s; [8]) and guinea pig cochlear Deiters' cells (~12 s [9]). However, the second phase of ATP-induced desensitisation which occurs between ATP applications, was distinctly different in the current mouse RM epithelial cell study [8]. In the guinea pig study, repeated ATP applications produced a substantial increase in time constant for desensitisation (increasing from 10 to 23 s), whereas in the mouse RM cells, the opposite was evident (decreasing from 8 to 3 s). This second time constant is very fast for a confirmed homomeric $P2X_2$ receptor and even approaches the primary ATP response desensitisation time constant in rat primary auditory neurons of ~2 s, where the ion channel was composed of a novel $P2X_{2-3}/P2X_3$ heteromer [17]. The principal determinant for this key difference in secondary desensitisation between the guinea pig RM epithelial cell $P2X_2$ receptor and the mouse RM epithelial cell $P2X_2$ receptor is likely to be the $P2X_{2-2}$ (P2X2b) splice variant, which was absent in the guinea pig. This perhaps reflect different evolutionary strategies to arrive at a common functional outcome, suggesting an important biological function for the channel.

Studies have demonstrated that alternative splicing of the $P2X_2$ receptor subunit generates subunit isoforms that contribute faster desensitisation than the full-length $P2X_2$ receptor (P2X2a) [16, 28–31]. As a result, the presence of splice variants were investigated in mouse RM epithelial cells. Here, RT-PCR analysis confirmed $P2X_2$ receptor mRNA transcript expression in Reissner's membrane epithelial cells for both the full-length P2X2a receptor and the splice variant P2X2b ($P2X_{2-2}$). This is in contrast to guinea pig RM epithelial cells which express the P2X2a mRNA transcript, but not the P2X2b isoform [8]. The P2X2b isoform lacks a series of C-terminal 69 amino acids and forms a functional homomeric ATP-gated channel which desensitises more rapidly than the full-length P2X2a isoform [15, 16, 29, 32]. This P2X2b splice variant and others has been detected in various guinea pig and rat cochlear tissues [15, 16, 22]. P2X2a and/or P2X2b expression have been detected in individual neonatal rat OHC [33], which have previously been shown to form functional heteromultimers with an intermediary rate of desensitisation [32]. It is likely that mouse RM epithelial cells express a full-length P2X2a/ P2X2b heteromer as the desensitisation time constant reported here for initial ATP-induced responses approaches that of the P2X2b variant, with an even faster time constant detected for subsequent ATP-activated current responses.

The increased rate of desensitisation of the mouse RM epithelial cell ATP-activated inward current with repeated activation is likely to be mediated by intracellular signalling. Highly variable rates of desensitisation of $P2X_2$ receptor currents have been observed in *Xenopus* oocytes (time constant from 4 to 1000 s) and HEK293 cells (time constant from 4 to 40 s), with a reduction in variability around an ~8 s time constant occurring when recording from outside-out patches pulled from oocytes, or alteration of an intracellular C-terminal region residue [34]. This indicated that intracellular components were required to maintain the channels in the slow desensitising form. Results here suggested that the P2X2b transcript may be less abundant than the full-length P2X2a transcript. It may be possible that repeated ATP applications in mouse RM epithelial cells changes the profile of the ATP-gated channels inserted in the membrane, with an increase in the proportion of faster desensitising P2X2b subunit within the P2X trimer. Expression studies using P2X-GFP reporter gene chimaeras indicate that the receptors are in dynamic flux within cells, and respond to agonist binding by changes in receptor clustering and receptor turnover [24, 35, 36]. Modification of phosphorylation sites in the amino and carboxy terminii has been shown to enhance desensitisation of $P2X_2$ receptors. $P2X_2$ receptor mutants with a disrupted intracellular N-terminal region PKC site display rapidly desensitising kinetics and were not potentiated by PKC activators, indicating that PKC phosphorylation can regulate the channel [37]. Modulators of other protein kinases have also been shown to affect $P2X_2$ receptor function [9, 38, 39]. Fujiwara and Kubo [40] demonstrated that phosphoinositide-3 kinase inhibition increased the rate of $P2X_2$ desensitisation by modulating phosphoinositide interaction with the $P2X_2$ C-terminal domain.

As noted above, the unusual kinetics of the channel appears to have high functional relevance. The desensitisation kinetics of the $P2X_2$ receptor could be one of the critical determinants for receptor responsiveness to repeating or continuous stimulations by ATP. Generating fast desensitising variants might limit $P2X_2$ receptor-mediated responses. This is of particular interest in the cochlea in terms of the ability of the ATP-activated cochlear partition conductance shunt being able to extend the dynamic range of hearing and to protect the cochlea from loud sound. Accumulation of ATP in the endolymphatic compartment arising from high level acoustic stimulation is likely to cause $P2X_2$ receptor-mediated desensitisation that slows the kinetics of the fall in the endocochlear potential and hence contributes to purinergic adaptation of sound transduction.

In summary, we have characterised the membrane conductance properties of mouse RM epithelial cell ATP-gated ion channels assembled from $P2X_2$ receptor subunits. This native homomeric $P2X_2$ receptor displayed comparatively fast desensitisation and exhibited a novel agonist-mediated increased rate of desensitisation. This likely reflects subunit complexity established by alternative splicing and contributes significantly to cochlear function.

Acknowledgments Supported by National Health and Medical Research Council of Australia grants 630618 and 1089838 (G.H., A.R.); the Health Research Council of New Zealand (G.H., P.T., S.V., A.R.) and Deafness Research Foundation of New Zealand (P.T., G.H., S.V.); James Cook Fellowship (Royal Society of New Zealand) (G.H.) and the VA Research Service 1I01BX001205-03 and NIH grant RO1 DC000139-26 (A.R.). Dr. Baljit Khakh is thanked for supporting early aspects of the study.

Competing interests The authors declare that they have no competing interests.

Authors' contributions GH designed the experiments with AR, SV and PT. RM-J contributed the majority of the cellular electrophysiology, supported by GH. DC provided ongoing support of the mouse models. RM-J and GH wrote the paper with participation from all authors. All authors read and approved the final manuscript.

References

1. North RA (2002) Molecular physiology of P2X receptors. Physiol Rev 82(4):1013–1067
2. Jiang LH, Kim M, Spelta V, Bo X, Surprenant A, North RA (2003) Subunit arrangement in P2X receptors. J Neurosci 23(26):8903–8910
3. Khakh BS, North RA (2006) P2X receptors as cell-surface ATP sensors in health and disease. Nature 442(7102):527–532
4. North RA, Surprenant A (2000) Pharmacology of cloned P2X receptors. Annu Rev Pharmacol Toxicol 40:563–580. doi:10.1146/annurev.pharmtox.40.1.563
5. Housley GD, Jagger DJ, Greenwood D, Raybould NP, Salih SG, Jarlebark LE, Vlajkovic SM, Kanjhan R, Nikolic P, Munoz DJ, Thorne PR (2002) Purinergic regulation of sound transduction and auditory neurotransmission. Audiol Neurootol 7(1):55–61
6. Housley GD, Bringmann A, Reichenbach A (2009) Purinergic signaling in special senses. Trends Neurosci 32(3):128–141
7. Housley GD, Morton-Jones R, Vlajkovic SM, Telang RS, Paramananthasivam V, Tadros SF, Wong AC, Froud KE, Cederholm JM, Sivakumaran Y, Snguanwongchai P, Khakh BS, Cockayne DA, Thorne PR, Ryan AF (2013) ATP-gated ion channels mediate adaptation to elevated sound levels. Proc Natl Acad Sci USA 110(18):7494–7499. doi:10.1073/pnas.1222295110
8. King M, Housley GD, Raybould NP, Greenwood D, Salih SG (1998) Expression of ATP-gated ion channels by Reissner's membrane epithelial cells. Neuroreport 9(11):2467–2474
9. Chen C, Bobbin RP (1998) P2X receptors in cochlear Deiters' cells. Br J Pharmacol 124(2):337–344
10. Jarlebark LE, Housley GD, Raybould NP, Vlajkovic S, Thorne PR (2002) ATP-gated ion channels assembled from P2X2 receptor subunits in the mouse cochlea. Neuroreport 13(15):1979–1984
11. Salih SG, Jagger DJ, Housley GD (2002) ATP-gated currents in rat primary auditory neurones in situ arise from a heteromultimetric P2X receptor subunit assembly. Neuropharmacology 42(3):386–395
12. Lee JH, Chiba T, Marcus DC (2001) P2X2 receptor mediates stimulation of parasensory cation absorption by cochlear outer sulcus cells and vestibular transitional cells. J Neurosci 21(23):9168–9174
13. Kanjhan R, Raybould NP, Jagger DJ, Greenwood D, Housley GD (2003) Allosteric modulation of native cochlear P2X receptors: insights from comparison with recombinant P2X2 receptors. Audiol Neurootol 8(3):115–128, **doi:69478**
14. Housley GD, Greenwood D, Bennett T, Ryan AF (1995) Identification of a short form of the P2xR1-purinoceptor subunit produced by alternative splicing in the pituitary and cochlea. Biochem Biophys Res Comm 212(2):501–508. doi:10.1006/bbrc.1995.1998
15. Brändle U, Spielmanns P, Osteroth R, Sim J, Surprenant A, Buell G, Ruppersberg JP, Plinkert PK, Zenner HP, Glowatzki E (1997) Desensitization of the $P2X_2$ receptor controlled by alternative splicing. FEBS Lett 404(2–3):294–298
16. Parker MS, Larroque ML, Campbell JM, Bobbin RP, Deininger PL (1998) Novel variant of the P2X2 ATP receptor from the guinea pig organ of Corti. Hear Res 121(1–2):62–70
17. Greenwood D, Jagger DJ, Huang LC, Hoya N, Thorne PR, Wildman SS, King BF, Pak K, Ryan AF, Housley GD (2007) P2X receptor signaling inhibits BDNF-mediated spiral ganglion neuron development in the neonatal rat cochlea. Development 134(7):1407–1417
18. Yan D, Zhu Y, Walsh T, Xie D, Yuan H, Sirmaci A, Fujikawa T, Wong AC, Loh TL, Du L, Grati M, Vlajkovic SM, Blanton S, Ryan AF, Chen ZY, Thorne PR, Kachar B, Tekin M, Zhao HB, Housley GD, King MC, Liu XZ (2013) Mutation of the ATP-gated P2X2 receptor leads to progressive hearing loss and increased susceptibility to noise. Proc Natl Acad Sci USA 110(6):2228–2233. doi:10.1073/pnas.1222285110
19. Faletra F, Girotto G, D'Adamo AP, Vozzi D, Morgan A, Gasparini P (2014) A novel P2RX2 mutation in an Italian family affected by autosomal dominant nonsyndromic hearing loss. Gene 534(2):236–239. doi:10.1016/j.gene.2013.10.052
20. Moteki H, Azaiez H, Booth KT, Hattori M, Sato A, Sato Y, Motobayashi M, Sloan CM, Kolbe DL, Shearer AE, Smith RJ, Usami S (2015) Hearing loss caused by a P2RX2 mutation identified in a MELAS family with a coexisting mitochondrial 3243AG mutation. Ann Otol Rhinol Laryngol 124(Suppl 1):177S–183S. doi:10.1177/0003489415575045
21. Cockayne DA, Dunn PM, Zhong Y, Rong W, Hamilton SG, Knight GE, Ruan HZ, Ma B, Yip P, Nunn P, McMahon SB, Burnstock G, Ford AP (2005) P2X2 knockout mice and P2X2/P2X3 double knockout mice reveal a role for the P2X2 receptor subunit in mediating multiple sensory effects of ATP. J Physiol 567(Pt 2):621–639
22. Salih SG, Housley GD, Burton LD, Greenwood D (1998) $P2X_2$ receptor subunit expression in a subpopulation of cochlear type I spiral ganglion neurones. Neuroreport 9(2):279–282
23. Yeh TH, Tsai MC, Lee SY, Hsu MM, Tran Ba Huy P (1997) Stretch-activated nonselective cation, Cl^- and K^+ channels in apical membrane of epithelial cells of Reissner's membrane. Hear Res 109(1–2):1–10
24. Khakh BS (2001) Molecular physiology of P2X receptors and ATP signalling at synapses. Nat Rev Neurosci 2(3):165–174
25. Gever JR, Cockayne DA, Dillon MP, Burnstock G, Ford AP (2006) Pharmacology of P2X channels. Pflugers Arch 452(5):513–537
26. Thorne PR, Munoz DJ, Housley GD (2004) Purinergic modulation of cochlear partition resistance and its effect on the endocochlear potential in the guinea pig. J Assoc Res Otolaryngol 5:58–65
27. Brake AJ, Wagenbach MJ, Julius D (1994) New structural motif for ligand-gated ion channels defined by an ionotropic ATP receptor. Nature 371(6497):519–523
28. Brandle U, Spielmanns P, Osteroth R, Sim J, Surprenant A, Buell G, Ruppersberg JP, Plinkert PK, Zenner HP, Glowatzki E (1997) Desensitization of the P2X(2) receptor controlled by alternative splicing. FEBS Lett 404(2–3):294–298
29. Simon J, Kidd EJ, Smith FM, Chessell IP, Murrell-Lagnado R, Humphrey PP, Barnard EA (1997) Localization and functional expression of splice variants of the P2X2 receptor. Mol Pharmacol 52(2):237–248
30. Koshimizu T, Tomic M, Koshimizu M, Stojilkovic SS (1998) Identification of amino acid residues contributing to desensitization of the $P2X_2$ receptor channel. J Biol Chem 273(21):12853–12857

31. Koshimizu TA, Tsujimoto G (2006) Functional role of spliced cytoplasmic tails in P2X2-receptor-mediated cellular signaling. J Pharmacol Sci 101(4):261–266
32. Koshimizu TA, Kretschmannova K, He ML, Ueno S, Tanoue A, Yanagihara N, Stojilkovic SS, Tsujimoto G (2006) Carboxyl-terminal splicing enhances physical interactions between the cytoplasmic tails of purinergic P2X receptors. Mol Pharmacol 69(5): 1588–1598. doi:10.1124/mol.105.019802
33. Brändle U, Zenner HP, Ruppersberg JP (1999) Gene expression of P2X-receptors in the developing inner ear of the rat. Neurosci Lett 273(2):105–108
34. Zhou Z, Monsma LR, Hume RI (1998) Identification of a site that modifies desensitization of P2X2 receptors. Biochem Biophys Res Comm 252(3):541–545
35. Dutton JL, Poronnik P, Li GH, Holding CA, Worthington RA, Vandenberg RJ, Cook DI, Barden JA, Bennett MR (2000) P2X(1) receptor membrane redistribution and down-regulation visualized by using receptor-coupled green fluorescent protein chimeras. Neuropharmacology 39(11):2054–2066
36. Chaumont S, Compan V, Toulme E, Richler E, Housley GD, Rassendren F, Khakh BS (2008) Regulation of P2X2 receptors by the neuronal calcium sensor VILIP1. Sci Signal 1(41):ra8
37. Boue-Grabot E, Archambault V, Seguela P (2000) A protein kinase C site highly conserved in P2X subunits controls the desensitization kinetics of P2X(2) ATP-gated channels. J Biol Chem 275(14): 10190–10195
38. Chow YW, Wang HL (1998) Functional modulation of P2X2 receptors by cyclic AMP-dependent protein kinase. J Neurochem 70(6):2606–2612
39. Xu GY, Huang LY (2004) Ca2+/calmodulin-dependent protein kinase II potentiates ATP responses by promoting trafficking of P2X receptors. Proc Natl Acad Sci USA 101(32):11868–11873. doi:10.1073/pnas.0401490101
40. Fujiwara Y, Kubo Y (2006) Regulation of the desensitization and ion selectivity of ATP-gated P2X2 channels by phosphoinositides. J Physiol 576(Pt 1):135–149. doi:10.1113/jphysiol.2006.115246